Nuclear effects in electron reactions and their impact on neutrino processes

Cite as: AIP Conference Proceedings **1189**, 115 (2009); https://doi.org/10.1063/1.3274140
Published Online: 02 December 2009

Maria B. Barbaro, J. E. Amaro, J. A. Caballero, R. Cenni, T. W. Donnelly, A. Molinari, and J. M. Udías

Nuclear effects in electron reactions and their impact on neutrino processes

Maria B. Barbaro*, J.E. Amaro†, J.A. Caballero**, R. Cenni‡, T.W. Donnelly§, A. Molinari* and J.M. Udías¶

*Turin University and INFN, Italy
†University of Granada, Spain
**University of Sevilla, Spain
‡INFN, Sezione di Genova, Italy
§M.I.T., Boston, USA
¶Universidad Complutense de Madrid, Spain

Abstract. We suggest that superscaling in electroweak interactions with nuclei, namely the observation that the reduced electron-nucleus cross sections are to a large degree independent of the momentum transfer and of the nuclear species, can be used as a tool to obtain precise predictions for neutrino-nucleus cross sections in both charged and neutral current-induced processes.

Keywords: Neutrino scattering, Electron scattering, Superscaling
PACS: 25.30.Pt, 23.40.Bw, 24.10.Jv

INTRODUCTION

The original idea of scaling in inclusive electron-nucleus scattering dates back to 1975, with the seminal work of West [1], and was further developed in Refs. [2, 3, 4, 5]. It basically states that at high momentum transfer (q larger than about 0.5 GeV/c) the ratio between the nuclear and single-nucleon cross sections does not depend on two variables (q, ω) but only on one scaling variable (y in a non-relativistic context and ψ in a relativistic framework). Another type of scaling (the so-called "second kind scaling") concerns the dependence of the above ratio upon the specific target and it is realized if the latter is inversely proportional to the Fermi momentum k_F. When both kinds of scaling are fulfilled, namely when the function

$$f = k_F \frac{\frac{d\sigma}{d\Omega d\omega}}{Z\sigma_{ep} + N\sigma_{en}} \tag{1}$$

does not vary with the momentum transfer q and with the nuclear target, one has "superscaling" and f is called superscaling function. Careful analyses of the (e,e') world data have shown that superscaling is working to a high degree of accuracy at the left of the quasielastic peak (QEP) and that its violations, occurring at the right of the QEP, reside in the transverse channel and are mainly (but not only) due to the excitation of a Δ-resonance. A similar analysis was recently performed in the region above the QEP [6, 7] and it was shown that also here superscaling is fulfilled, although to a lesser degree of accuracy, providing an appropriate dividing factor and scaling variable, both accounting for the Δ-nucleon mass difference, are used.

As a consequence a good representation of the electromagnetic response can be obtained in both the quasielastic and Δ regions by embodying the nuclear effects in two phenomenological superscaling functions, as will be illustrated in the next Section.

The scaling approach can then be inverted and predictions can be made for neutrino reactions by multiplying the superscaling function by the appropriate single nucleon neutrino factors. This approach, referred to as "SuSA" (SuperScaling Approximation) and illustrated in Section 3, has the merit of minimizing the model dependence implicitly associated to any direct calculation of neutrino-nucleus cross sections, because the complexity of the nuclear dynamics is extracted by the experimental electron scattering data. It also has limitations related to the quality of superscaling: it cannot be applied to very low momentum transfer, where nuclear collective effects become important, and it neglects the contribution of meson exchange currents which, being carried by two-body operators, are breaking both kinds of scaling. We will shortly comment on these scaling violations in Section 4.

CP1189, *From Sixth International Workshop on Neutrino-Nucleus Interactions in the Few-GeV Region*,
edited by F. Sanchez, M. Sorel, L. Alvarez-Ruso, A. Cervera, and M. Vicente-Vacas

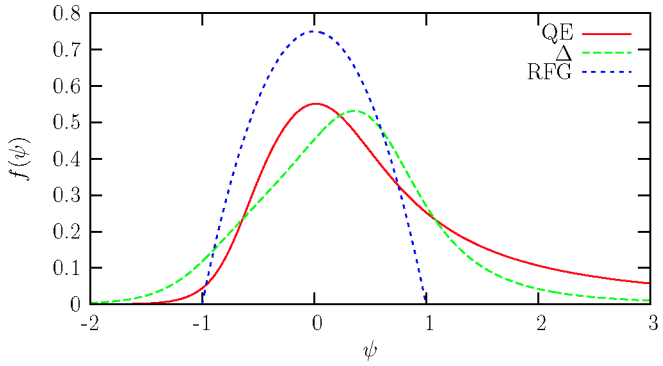

FIGURE 1. The phenomenological QE (solid, red on-line) and Δ (dashed, green on-line) superscaling functions compared with the RFG result (dotted, blue on-line).

THE SUPERSCALING FUNCTIONS IN INCLUSIVE ELECTRON SCATTERING

By applying the procedure outlined in the previous section (see Refs. [4, 5, 8, 6] for details), the two scaling functions shown in Fig. 1, to be used in the QE and Δ peak regions respectively, can be extracted from the data. In Fig. 1 the Relativistic Fermi Gas (RFG) result, corresponding to the parabola $f = \frac{3}{4}(1-\psi^2)$, is also shown for comparison.

Note that both phenomological superscaling functions present an asymmetric shape with a pronounced tail extending into the region of high transferred energies, corresponding to positive values of the scaling variable ψ. This tail is absent in the RFG result, which is symmetric in ψ. While this asymmetry is largely absent in most non-relativistic models based on the impulse approximation, it has been shown that the correct amount of asymmetry for the QE superscaling function is provided within a few models:

1. the relativistic impulse approximation when final state interactions (FSI) are described with a relativistic mean field (RMF) potential [9],
2. a semi-relativistic model including FSI through a Dirac-equation-based model [10],
3. a covariant extension of the relativistic Fermi gas model which incorporates correlation effects in nuclei in analogy to the BCS descriptions of systems of fermions [11].

This is illustrated in Figs. 2 and 3. In Fig. 2 the RMF quasielastic scaling function is compared with the data and with other relativistic models (the Relativistic Plane Wave Impulse Approximaton and a Relativistic Optical Model using a real relativistic potential), which are clearly unable to reproduce the high energy tail. In Fig. 3 the "BCS-like" scaling function is plotted for different values of a parameter β, which controls the slope of the momentum distribution (see Ref. [11] for details): it clearly appears that the model has the capability of reproducing the experimental data providing the nucleon momentum distribution displays a sufficiently large high-momentum tail (corresponding to low values of β). The connection between the nucleon's momentum distribution and the scaling function and its application to neutrino reactions have also been explored in Refs. [12, 13, 14] within the Coherent Density Fluctuation Model.

The microscopic origin of the difference between the two functions displayed in Fig.1 has been recently explored in Ref. [7] but relativistic theoretical models for the Δ-resonance region are still missing, so that the present phenomenological approach is probably the most reliable one in this kinematical domain.

With the above ingredients, it is then possible to recalculate for every nucleus, incident electron energy and scattering angle the inclusive cross section for energy transfers ω below the maximum of the Δ contribution. In order to illustrate this, in Fig. 4 we show the experimental cross section together with the calculated response obtained using the parameterized superscaling functions for a particular kinematics. A variety of different kinematics has been explored in Ref. [6] for ^{12}C and ^{16}O, since these are the relevant nuclei for the MiniBooNE and K2K/T2K neutrino oscillation measurements. For the data sets which do cover the Δ region, typical deviations are 10% or less, whereas the RFG model clearly fails to reproduce the data, especially in the "dip" region between the two peaks.

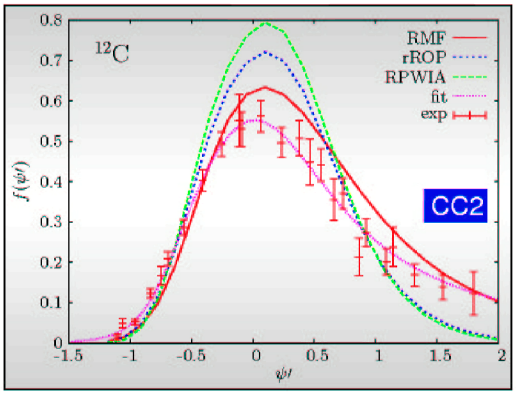

FIGURE 2. The QE superscaling function f evaluated in different relativistic models (see text) and compared with the experimental data. The scaling variable ψ' includes a small phenomenological energy shift needed in order to adjust the position of the QEP to the data.

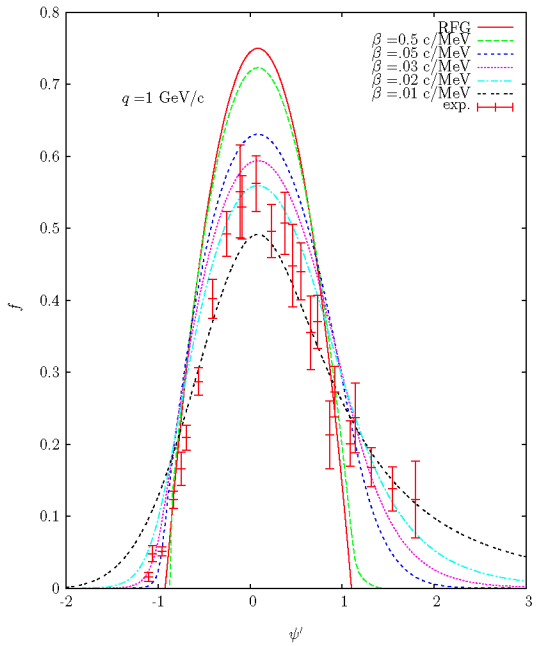

FIGURE 3. The "BCS-like" QE scaling function (see Ref. [11]) evaluated for different choices of the parameter β controlling the momentum distribution and compared with the data and the RFG result.

THE SUSA MODEL: PREDICTIONS FOR NEUTRINO CROSS SECTIONS

In this Section we present some results obtained within the superscaling approach for neutrino-nucleus charged and neutral current induced processes.

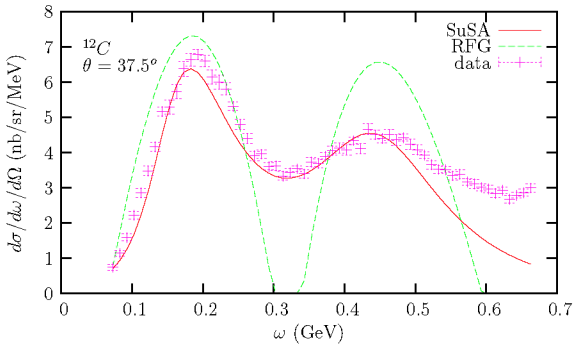

FIGURE 4. Electron scattering data (from Ref. [15]) compared with the SuSA (solid, red on-line) and RFG (dashed, green on-line) calculations.

Charged Current reactions

According with what previously illustrated we can evaluate the cross sections relative to the charged current (CC) process, where a lepton l is detected in the final state, by multiplying the phenomenological superscaling function by the corresponding $\nu_l + n \rightarrow l^- + p$ cross section. We refer the reader to Ref. [6] for further details; here we just remind that we use the Hoehler parameterization [16] for the vector form factors and a dipole axial form factor with a cutoff mass $M_A = 1.032$ MeV.

In Fig. 5 we display for illustration the double differential cross section of neutrino scattering off ^{12}C with respect to the outgoing muon momentum k' and solid angle Ω for fixed muon scattering angle $\theta = 90^o$ and neutrino momentum k=1 GeV/c. The latter is chosen as representative of the kinematics where the scaling approach is expected to work well. Results corresponding to different nuclei and kinematics as well as to antineutrino scattering can be found in Ref. [6]. Note that the quasi-elastic and Δ peaks have roughly the same heighth for this kinematics, although this changes with the scattering amgle. Note also that the predictions at low momenta k', to the left of the Δ peak, are not reliable because our scaling approach does not fully account for meson production, resonances other than the Δ and deep inelastic scattering processes. Work aimed to include these contributions has been recently performed for electron scattering [7] and will be applied to neutrino scattering in future work.

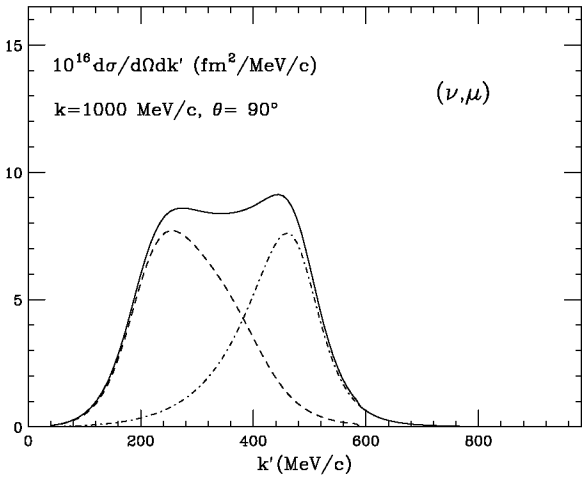

FIGURE 5. Double differential cross section for charged-current neutrino scattering plotted versus the muon energy for fixed neutrino energy and scattering angle. The separate Δ (left peak) and QE (right peak) contributions are displayed.

In order to assess the uncertainties related to different nuclear models, in Fig. 6 we plot the fully integrated cross section σ as a function of the incident neutrino energy as calculated within five different models [17]: the RMF, the Relativistic Plane Wave Impulse Approximation (RPWIA), the RFG, the SuSA model, and a semi-relativistic shell model [18] including (SRWS-tot) or not (SRWS) the contribution of the discrete spectrum of the residual nucleus ^{12}N obtained with the Woods-Saxon potential. We note that all of the descriptions lead to a similar behavior for the quasielastic cross section, which increases with the neutrino energy up to $\varepsilon_\nu \sim$ 1–1.2 GeV and then saturates to an

almost constant value. However, while the RPWIA, RFG, SRWS and SRWS-tot yield very similar results, the SuSA and RMF predictions are close to each other and significantly lower than the RFG. The reduction remains sizeable even at large ε_ν and tends to stabilize, being of the order of $\sim$15% at neutrino energies $\varepsilon_\nu \geq 1.2$ GeV.

Before concluding this Section, a comment is in order concerning the effect of Pauli blocking (PB). It is well-known that PB, which is obviously accounted for in the RFG model, only affects the low momentum and energy transfer region. However in the process we are considering here this region is kinematically forbidden due to the mass difference between the initial (^{12}C) and residual (^{12}N) nuclei. As a consequence the effect of PB in the integrated cross sections turns out to be negligible.

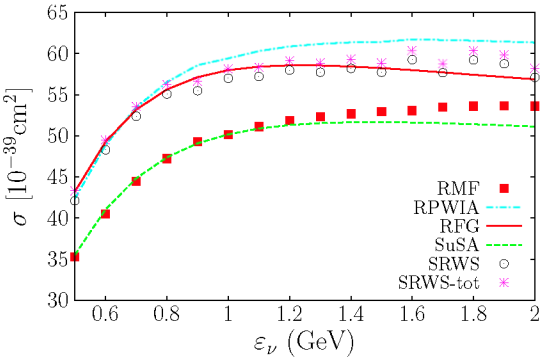

FIGURE 6. Charged-current neutrino cross section integrated over the muon energy and the scattering angle versus the neutrino energy (see text for the description of the various curves).

Neutral Current reactions

For neutral current (NC) reactions, e.g., $^{12}C(\nu,p)\nu X$, a new feature arises with respect to the CC case. Indeed in this case the scattered lepton is a neutrino and therefore not detected, but the knocked-out nucleon is detected: it is then the u-channel, rather than the t-channel, whose kinematics are controlled (see [19] for discussions of this case). Accordingly, in the scaling analysis it is not obvious that the process can be simply related to inclusive electron scattering, and therefore to apply the scaling ideas to NC neutrino and antineutrino scattering.

However it has been proven in Ref. [20] through a numerical analysis that the SuSA approach is still applicable. Indeed, as shown in Fig. 7, the exact RFG result (dotted blue curve) almost coincides with the one obtained under the factorization assumption which underlies superscaling (solid red). This outcome, closely related to the smooth variation of the single-nucleon factor inside the integration region, allows us to calculate NC cross sections using the SuSA model (dashed green). The SuSA cross sections are seen to be lower by about 25% at the peak than the RFG results, an effect similar to what was found for charge-changing processes. Moreover, the empirical scaling function leads to cross sections extending both below and above the kinematical region where the RFG is defined. In particular, the long tail displayed for low T_N-values (corresponding to positive values of the scaling variable ψ') is noteworthy. This tail arises not only from the asymmetric shape of the phenomenological scaling function, but also from the effective NC single-nucleon cross section, which increases significantly for low T_N values. We refer the reader to Ref. [20] for further results concerning neutron knockout, antineutrino scattering and the possibility of extracting information about the possible presence of strangeness in the nucleon from neutrino scattering data.

SCALING VIOLATIONS

Owing to the complexity of nuclear dynamics it is not obvious that the nuclear response to an electroweak field superscales. Indeed several effects are expected to break superscaling to some extent: off-shellness, collective nuclear excitations, meson-exchange currents (MEC), nucleon-nucleon (NN) correlations. To assess the impact of these contributions in the QE peak region is then of crucial importance. However a fully relativistic treatment of meson-exchange currents, which is required by the high energies involved in neutrino experiments, is a very demanding task because a large number of diagrams has to be taken into account, each of them involving multidimensional integrals. Moreover, in order to preserve gauge invariance not only the genuine meson exchange currents, where the virtual boson attaches to the meson, have to be calculated, but also the associated two-body correlation currents.

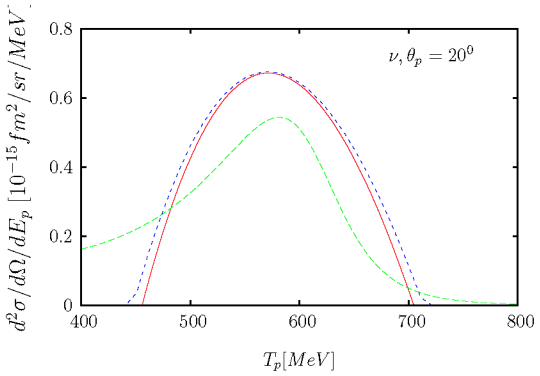

FIGURE 7. Quasielastic differential cross section for neutral current 1 GeV neutrino scattering from ^{12}C for proton knockout obtained using the RFG (dotted, blue on-line), the factorized approach with the RFG scaling function (solid, red on-line) and the phenomenological superscaling function (dashed, green on-line).

Progress in this directions has been made in the last years in a RFG framework, where the contribution of the pionic MEC to the QE responses have and the associated correlations can be exactly evaluated. The full calculation in the 1p-1h sector has been performed in Refs. [21, 22, 23], where it was shown that the MEC break scaling and that they are not negligible, yielding a depletion of the QEP of about 10-15%, depending on the kinematics. Moreover, delicate cancellations occur between the various contributions. Recently the same calculation has been performed in a semirelativistic shell model including final state interactions [24], where it is shown that new effects, absent in the RFG case, arise from the interplay between MEC and FSI.

In the 2p-2h sector the evaluation of the MEC contribution is very demanding from the computational point of view and a complete gauge invariant calculation is not yet available, although work is in rogress in this direction. From the results of Refs. [25], which include the pure MEC but not the associated correlation diagrams, it appears that these contributions are essential if one is to have a quantitative picture of inclusive electron scattering at the kinematics relevant for neutrino experiments.

REFERENCES

1. G. B. West, Phys. Rept. **18**, 263 (1975).
2. W. M. Alberico, A. Molinari, T. W. Donnelly, E. L. Kronenberg and J. W. Van Orden, Phys. Rev. C **38**, 1801 (1988);
3. D. B. Day, J. S. McCarthy, T. W. Donnelly and I. Sick, Ann. Rev. Nucl. Part. Sci. **40**, 357 (1990).
4. T.W. Donnelly and I. Sick, Phys. Rev. Lett. **82**, 3212 (1999).
5. T.W. Donnelly and I. Sick, Phys. Rev. C **60**, 065502 (1999).
6. J. E. Amaro, M. B. Barbaro, J. A. Caballero, T. W. Donnelly, A. Molinari and I. Sick, Phys. Rev. C **71**, 015501 (2005).
7. C. Maieron, J. E. Amaro, M. B. Barbaro, J. A. Caballero, T. W. Donnelly, and C. F. Williamson, in print on Phys. Rev. C, arXiv:0907.1841v1 [nucl-th].
8. J. Jourdan, Nucl. Phys. A **603**, 117 (1996).
9. J. A. Caballero, J. E. Amaro, M. B. Barbaro, T. W. Donnelly, C. Maieron and J. M. Udias, Phys. Rev. Lett. **95**, 252502 (2005).
10. J. E. Amaro, M. B. Barbaro, J. A. Caballero, T. W. Donnelly and J. M. Udias, Phys. Rev. C **75**, 034613 (2007).
11. M. B. Barbaro, R. Cenni, T. W. Donnelly and A. Molinari, Phys. Rev. C **78**, 024602 (2008); M. B. Barbaro, R. Cenni, T. W. Donnelly and A. Molinari, arXiv:0809.2744v1 [nucl-th]
12. A. N. Antonov, M. V. Ivanov, M. K. Gaidarov and E. Moya de Guerra, Phys. Rev. C **75**, 034319 (2007).
13. M. V. Ivanov, M. B. Barbaro, J. A. Caballero, A. N. Antonov, E. Moya de Guerra and M. K. Gaidarov, Phys. Rev. C **77**, 034612 (2008).
14. A. N. Antonov, M. V. Ivanov, M. B. Barbaro, J. A. Caballero, E. Moya de Guerra and M. K. Gaidarov, Phys. Rev. C **75**, 064617 (2007).
15. O. Benhar, D. Day and I. Sick, Rev. Mod. Phys. **80**, 189 (2008).
16. G. Höhler *et al.*, Nucl. Phys. B **114**, 505 (1976).
17. J. E. Amaro, M. B. Barbaro, J. A. Caballero and T. W. Donnelly, Phys. Rev. Lett. **98**, 242501 (2007).
18. J. E. Amaro, M. B. Barbaro, J. A. Caballero, T. W. Donnelly and C. Maieron, Phys. Rev. C **71**, 065501 (2005).
19. M. B. Barbaro, A. De Pace, T. W. Donnelly, A. Molinari and M. J. Musolf, Phys. Rev. C **54**, 1954 (1996).
20. J. E. Amaro, M. B. Barbaro, J. A. Caballero and T. W. Donnelly, Phys. Rev. C **73**, 035503 (2006).
21. J. E. Amaro, M. B. Barbaro, J. A. Caballero, T. W. Donnelly and A. Molinari, Nucl. Phys. A **697**, 388 (2002).

22. J. E. Amaro, M. B. Barbaro, J. A. Caballero, T. W. Donnelly and A. Molinari, Phys. Rept. **368**, 317 (2002).
23. J. E. Amaro, M. B. Barbaro, J. A. Caballero, T. W. Donnelly and A. Molinari, Nucl. Phys. A **723**, 181 (2003).
24. J. E. Amaro, M. B. Barbaro, J. A. Caballero, T. W. Donnelly, C. Maieron and J. M. Udias, arXiv:0906.5598 [nucl-th].
25. A. De Pace, M. Nardi, W. M. Alberico, T. W. Donnelly and A. Molinari, Nucl. Phys. A **726**, 303 (2003); Nucl. Phys. A **741**, 249 (2004).